

Airborne forest fire mapping with an adaptive infrared sensor

D. OERTEL, K. BRIESS, W. HALLE, M. NEIDHARDT,
E. LORENZ, R. SANDAU, F. SCHRANDT, W. SKRBEK,
H. VENUS, I. WALTER, B. ZENDER, B. ZHUKOV

DLR, Institut für Weltraumsensorik und Planetenerkundung, Rutherfordstr. 2,
12489 Berlin, Germany; e-mail: dieter.oertel@dlr.de

J. G. GOLDAMMER, A. C. HELD, M. HILLE

Max Planck Institute for Chemistry/The Global Fire Monitoring Center,
Freiburg, PO Box 79085, Freiburg, Germany

and H. BRUEGGEMANN

SCANDAT, Arnfriedstr. 17, 12683 Berlin, Germany

(Received 22 November 2001; in final form 15 July 2002)

Abstract. The international scientific community has called for more detailed data on vegetation fires to improve the understanding of their role in global atmospheric chemistry, and on fire itself as an ecosystem disturbance. The fire science community highlighted the value of information such as fire spatial distribution, timing, extent, energy release, burning efficiency and emissions. In order to obtain reliable information on these parameters, a combination of operational and experimental space-borne sensors with *in situ* and airborne sensor measurements is required. A small satellite demonstrator mission on Bi-spectral InfraRed Detection (BIRD) was prepared by the Institute of Space Sensor Technology and Planetary Exploration of the German Aerospace Center (DLR). It was successfully launched on 22 October 2001 into a 570 km sun-synchronous orbit. This paper presents new thermal mapping results obtained with the Advanced BIRD Airborne Simulator (ABAS) during a flight campaign over controlled forest fires in the open coal mining region of the Brandenburg country in Germany on 23 August 2001. These data have been successfully used to retrieve the effective area and effective temperature of forest fires by means of the application of the bi-spectral sub-pixel method.

1. Introduction

Studies on tropospheric chemistry and meteorology have shown that vegetation fires and volcano emissions account for a substantial amount of photochemical oxidants and haze over the high temperature event region. Vegetation fires and volcano eruptions affect the chemistry of the atmosphere, alter the radiation budget of the Earth, and contribute to the greenhouse process through gases such as CO₂, CH₄, and N₂O. An increase of anthropogenic vegetation fires with subsequent loss of vegetation cover and site degradation also contributes to a change of global climate.

Current space-borne sensor systems are used to generate products of fire susceptibility evaluating time-series of vegetation state data, occurrence and coarse location of active fires, as well as smoke and burnt areas (fire scars). However, existing and planned operational space-borne sensors show serious limitations (e.g. part channel saturation leading to reduced high temperature event discrimination, spatial resolution more than 1 km) if accurate geophysical parameters—such as fire temperature, area and emissions—have to be obtained (Ahern *et al.* 2001). As a result, they allow only detection of larger fires with an area typically larger than 0.1 Ha. The corresponding algorithms are well developed for Advanced Very High Resolution Radiometer (AVHRR; e.g. Flannigan and Von der Haar 1986, Kaufman *et al.* 1990, Lee and Tag 1990, Franca *et al.* 1995, Flasse and Ceccato 1996, Justice *et al.* 1996, Li *et al.* 1997, Pereira and Setzer 1993, Pozo *et al.* 1997, Rauste *et al.* 1997, Arino and Melinotte 1998, Randriambelo *et al.* 1998, Giglio *et al.* 1999), GOES (Prins and Menzel 1992, Prins *et al.* 1998), DMSP (Cahoon *et al.* 1992), and MODIS (Kaufman *et al.* 1998). Only the low-sensitive ‘fire channel’ of MODIS allows a quantitative characterization of larger fires in terms of radiative energy release. Retrievals of fire temperature and area from the MODIS data are usually unstable due to its low resolution (Giglio and Kendall 2001, Wooster *et al.* 2001).

In order to close these ‘gaps’ in fire remote sensing the German Aerospace Center (DLR) prepared a space-borne precursor fire mission: the Bi-spectral infrared (IR) Detection (BIRD) small satellite mission, which is a technology demonstrator of new infrared push-broom sensors dedicated to the recognition and quantitative characterization of high temperature events (HTE) on the surface of the Earth.

The starting point of the BIRD development was the successful completion of the feasibility study for a Fire Recognition System for Small Satellites (FIRES 1994).

This study reveals that both the global change scientific community and the disaster management authorities expect from new and dedicated space-borne fire observation sensors spatial resolutions of 50–100 m for local observations, and a few hundred metres for global observations, as well as the ability for quantitative estimation of fire parameters such as:

- geo-location (with an accuracy better than 0.5 km);
- surface extent and intensity (temperature and energy release) of fire events;
- frequency of fire occurrence; and
- associated aerosol and trace gas emissions.

A new Hot Spot Recognition System, based on IR push-broom sensors, has been developed at DLR for the BIRD satellite mission and for an Advanced BIRD Airborne Simulator (ABAS). It will allow new data to be obtained for fire research.

2. The Brandenburg fire experiment

A controlled forest fire experiment was conducted in the vicinity of Cottbus, Germany, on 23 August 2001. Its main aim was to develop a model for the burning characteristics of the pine forest in the Brandenburg region, where wildfires happen most frequently in Germany.

The experiment was carried out by the German Research Network of Natural Disasters (Deutsches Forschungsnetz Naturkatastrophen) which includes a work package ‘Early Warning, Monitoring, Information Management and Simulation of

Forest Fire Danger' (DFNK 2001). The work package aims to develop a Geo Information System (GIS)-based information system which will include early warning, monitoring, information management and simulation of forest fire danger (including long-term forecasts). A prototype system will be implemented in the south-eastern part of the state of Brandenburg, Germany. The work package is also an activity of the Fire Ecology Research Group/Global Fire Monitoring Center (GFMC) of the Max Planck Institute for Chemistry (GFMC 2001).

A number of research institutions were involved in the multidisciplinary fire experiment which included, among other things, testing of a fire behaviour model (Max Planck Institute for Chemistry), a fire-weather component (German Weather Service), fire emissions measurements (Max Planck Institute for Chemistry), testing of the tower-based Automated System for Early Forest Fire Detection (Automatisiertes Waldbrand-Früherkennungssystem—AWFS) of the DLR (Kührt *et al.* 2000), and testing of ABAS conducted by DLR and SCANDAT.

The experiment took place on the territory of the Lausitzer Bergbau Aktien Gesellschaft (LAUBAG) where preparatory measures for a new open coal mining have been conducted.

3. Location and characteristics of the test site

The test site is located near Cottbus (51° 47' 03" N, 14° 24' 20" E), comprises four plots, and it has a total size of 2 ha of Scotch Pine (*Pinus sylvestris* L.) stands. The plots consisted of groups with trees of various ages ranging from 15 to 100 years and an inhomogeneous cover of grasses (*Calamagrostis epigeios* L. and *Deschampsia flexuosa* L.).

Table 1 provides an overview of fuel loads classified in accordance with the US National Fire Danger Rating System (USA) (Deeming *et al.* 1977).

Figure 1 shows the test site with the marked four experimental burning plots (I–IV).

4. Requirements to sensors for remote detection and thermal mapping of fire

The temperature of vegetation fires depends on the type of combustion and ranges from 500 K (smouldering combustion) to 1200 K (flaming combustion). The maximum in the spectral radiance distribution of the vegetation fires occurs in the mid wave infrared (MWIR) region at 3–5 μm . Therefore, the mid wave infrared spectral range is commonly recognized as the optimal spectral range for satellite fire detection (e.g. Robinson 1991). Reflected solar radiation and background thermal emission are relatively low in the MWIR for land surfaces. Nevertheless, using only

Table 1. Fuel loads in the experimental plots I to IV. Fuels are classified by timelag classes. The 1000-hr class is divided into partly decayed (pd) and non-decayed (nd).

Plot	Humus layer (cm)	Fuels (t ha^{-1}) (Grass and woody fuels by timelag classes)						Total
		Grass	1	10	100	1000 nd	1000 pd	
I	1.8	0.06	0.69	2.35	1.23	0.00	2.15	6.41
II	1.6	0.09	1.10	1.50	6.13	1.74	0.65	11.12
III	1.9	1.8	0.40	2.11	16.08	6.16	3.56	13.31
IV	1.3	0.05	0.36	1.50	2.69	0.00	1.68	6.23

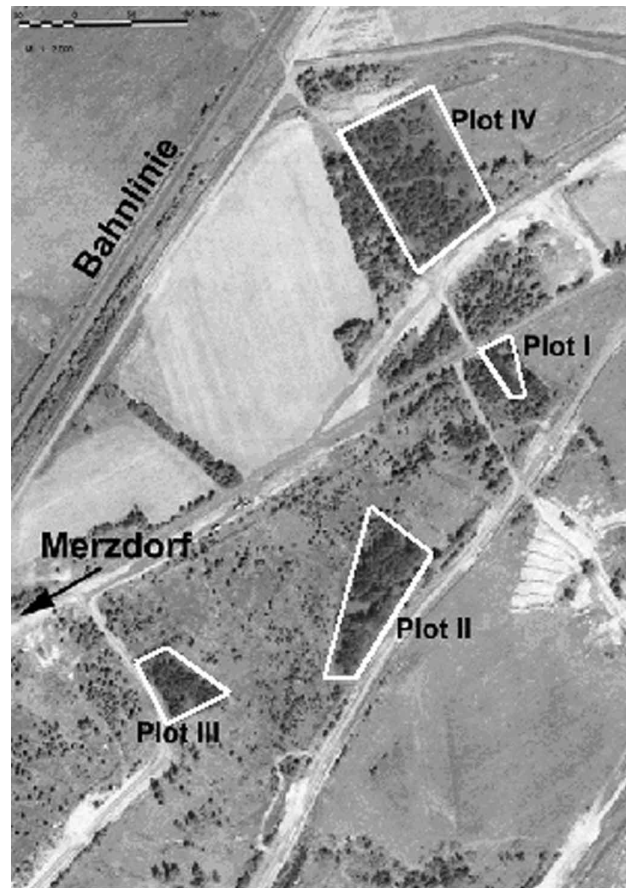


Figure 1. Test site with the marked Plots I–IV.

the MWIR channel for remote fire recognition may lead to false alarms generated by sun glints from water surfaces, building roofs and clouds or by larger sun heated land surface areas not covered with vegetation ('warm surfaces'). These false alarms may be rejected (with the exception of strong sun glints) by increasing the MWIR detection threshold, although this results in missing smaller and colder (smouldering) fires.

Fires in their initial stage may occupy only a small portion of a pixel, making their signal comparable or even smaller than natural variations of the background signal. The detection of small forest fires from satellites (where the fire area might be less than 0.001 of the pixel area) requires a sufficiently high signal-to-noise ratio in the MWIR channel as well as a separation of fire signals from natural variations of the MWIR radiation. On the other hand, the sensor should not be saturated by a strong signal from large fires occupying the whole pixel. Therefore, a very large dynamic range in the MWIR of about 20 bits is required for this purpose, in order:

- to resolve in this band the 300 K background temperature with the temperature resolution of <0.3 K; and
- not to saturate from a 1200 K fire occupying the full pixel.

These requirements can be met using:

- cooled array detectors;
- sophisticated real-time detector signal processing; and
- on-board detector exposition time control.

Visible (VIS) and/or near infrared (NIR) channels must be co-registered to the MWIR and thermal infrared (TIR) channels for:

- the rejection of false alarms caused by sun glints and warm surfaces using a MWIR/VIS (or MWIR/NIR) and MWIR/TIR radiance ratio thresholding; and
- a reliable detection of fire scars in the NIR.

The main spectro-radiometric requirements to the channels of a multi-spectral imager for reliable fire detection and analysis are given in table 2.

Inter-channel geometric shifts should be corrected to an accuracy of ~ 0.2 of a MWIR/TIR pixel size to avoid a significant degradation of the fire detection capability (the minimal detectable fire area); otherwise detection thresholds should be increased to avoid false alarms caused by inter-channel miss-registration (Zhukov and Oertel 2001). A higher geometric correction accuracy of ~ 0.1 of a pixel size is required for the MWIR and TIR channels to provide temperature and area retrieval for sub-pixel fires by the bi-spectral technique (Dozier 1981) if it is applied at a pixel scale. This latter requirement is relaxed if the bi-spectral analysis is performed at the level of detected fire clusters since their MWIR and TIR radiation fluxes are rather insensitive to small geometric inter-channel shifts.

Inter-channel differences of the point spread function (PSF) lead to different spatial averaging in different channels and cause similar effects on fire detection and analysis as inter-channel shifts. As shown in Zhukov and Oertel (2001), the PSF width in different channels should be adjusted to an accuracy of $\sim 10\%$. Bi-spectral analysis at the level of fire clusters again is not sensitive to small inter-channel PSF errors.

5. The BIRD hot spot recognition sensor and airborne simulators

The development of airborne simulators for new space-borne sensors is a common approach, especially since new working principles of the future space-borne sensors must be tested experimentally before manufacturing of the space sensor begins.

The BIRD Airborne Simulator no. 1 (BAS 1) was developed in 1996 and tested in 1997–1998 before the flight and spare models of the BIRD Hot Spot Recognition

Table 2. Spectro-radiometric requirements for space-borne fire recognition.

Spectral region	Spectral coverage (μm)	Spectral resolution (μm)	Radiometric dynamic (bit)	Radiometric resolution
Mid wave infrared (MWIR)	3.4–4.3	~ 1.0	> 20	NEAT ¹ < 0.5 K
Thermal infrared (TIR)	8.5–9.3 or 10.5–11.7	~ 1.0	> 14	NEAT < 0.3 K
Visible (VIS)	0.63–0.70	0.05	> 8	SNR ² > 100
Near infrared (NIR)	0.77–0.80	0.03	> 8	SNR ² > 100

¹Noise equivalent temperature difference.

²Signal to noise ratio.

System (HSRS) sensors were finally constructed and manufactured at DLR Berlin. The main tasks of BAS 1 were:

- to test the latest generation of machine cooled IR-push-broom sensors based on cadmium mercury telluride (CMT) line arrays with staggered structure; and
- to test qualitatively the real-time processing and control of radiometric dynamic adaptation for the CMT line arrays between normal and high temperature targets in the observed scene.

The primary objective of HSRS—to measure fire temperature, area and energy release in a large dynamic range—requires a special technique for the scene sampling. Laboratory tests and laboratory calibration measurements are both an important part of HSRS development and its airborne validation strategy. However, only flight experiments with real fire scenes permit hidden problems to be revealed and allow the full capability of this new technique.

HSRS is a bi-spectral push-broom scanner with spectral bands in the MWIR at $3.9\ \mu\text{m}$ and TIR at $8.8\ \mu\text{m}$. The sensitive devices are two CMT photodiode lines. The lines, with identical layout in MWIR and TIR, comprise 2×512 elements each in a staggered structure.

These arrays have to be cooled to 100 K in MWIR and to 80 K in TIR. As the maximum achievable at 80 K TIR photodiode cut-off wavelength is at about $10\ \mu\text{m}$ and the atmospheric ozone band is at $9.6\ \mu\text{m}$, it is necessary to use the $8.5\text{--}9.3\ \mu\text{m}$ band for TIR channel of the HSRS instead of the commonly used $10.5\text{--}11.7\ \mu\text{m}$ band. The cooling must be conducted in a satellite mission by small Stirling cooling engines. HSRS sensor head components of both spectral channels are based on identical technologies to provide good pixel co-alignment. Both spectral channels have the same optical layout but with different wavelength-adapted lens coatings.

The HSRS sensor data are read out continuously with a clock time which is exactly one half the pixel dwell time. This time-controlled 'double sampling' and the staggered line array structure allow geometric resolution enhancement compared to a classic line array.

Radiometric fire measurements require a large dynamic range, as outlined above. To fulfil this requirement, a second scene sampling has to be performed with reduced exposure time (within the same sampling clock time interval!) if hot areas are identified during the real-time processing of the data from the first scene sampling. This second sampling is only performed if the real-time processing of the first sampling set indicates that detector elements are saturated or close to saturation. These supplementary sampled pixels are added to the normal thermal scene measurement data as the so called 'Hot Area (HA)' data sub-set. All these sampled data are transmitted to the HSRS data acquisition controller via a special serial interface. The HSRS has an adaptive radiometric dynamic range which allows the recognition of high temperature events (HTE) such as wildfires, volcanic activities, or coal seam fires without sensor saturation.

The Advanced BIRD Airborne Simulator (ABAS) was built based on the experiences obtained with BAS 1 (Skrbek and Lorenz 1998). It was completed at DLR Berlin in summer 2001 using the HSRS BIRD flight spare (which was possible only after the final BIRD IR-sensor pre-flight tests).

The geometric correction of multi-spectral push-broom sensor raw data is a serious task. The simultaneous registration of the aircraft attitude (at the sensor

heads) and of the aircraft position is necessary if it is intended that radiometrically and geometrically calibrated data are to be obtained.

ABAS provides radiometric and geometric calibrated bi-spectral IR imager data in combination with VIS/NIR charge coupled device (CCD) line data. The ABAS block-scheme is shown in figure 2.

ABAS comprises the following sensors/receivers:

- a push-broom Hot Spot Recognition Sensor (HSRS) for mid-wave IR (MWIR) and thermal IR (TIR);
- a wide angle airborne camera (WAAC) with changeable entrance filters for the visible or near IR (VIS/NIR);
- a 3-axis Fibre Gyro block; and
- a Global Positioning System (GPS) receiver.

Special features of the BIRD and ABAS HSRS are:

- cold shielding within the detector dewar;
- spectral range separation by coating of the dewar entrance window; and
- a fully dewar-detector-array adapted lens design is able to provide radiometric exact and calibrated data.

The ABAS VIS/NIR three-line CCD camera WAAC was derived from the wide angle optoelectronic stereo scanner (WAOSS) developed for the Mars 96 Mission.

WAAC is a three-line stereo scanner working in the push-broom mode. According to the camera design the stereo information is obtained within the image plane of a single wide-angle lens. Each of the three CCD lines has a different viewing direction: forward, nadir, and backward.

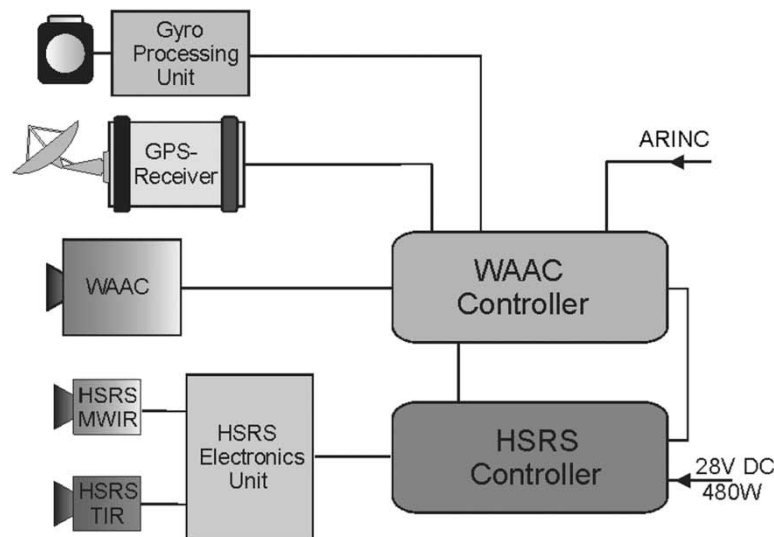


Figure 2. Block-scheme of the BIRD Airborne Simulator. ARINC=airborne inertial data.

The ABAS arrangement is separated in two main parts:

- A sensor platform with imaging sensors and gyro sensors, as shown in figure 3; and
- A 19" rack with WAAC and HSRS controller console, including a GPS receiver, as shown in figure 4.

Table 3 gives an overview of the main parameter of ABAS. Table 4 shows ABAS swath width/pixel sizes for three flight altitudes over ground.

Flown at $h=3000$ m over ground ABAS can deliver data which will allow the use of sub-pixel recognition routines (after radiometric calibration, geometric data correction and co-registration processing):

- to detect a 800 K fire with an area $>80\text{ cm}^2$ and a 500 K fire with an area $>1000\text{ cm}^2$; and
- to provide an effective fire temperature retrieval accuracy of better than 10% and an effective fire area retrieval accuracy of 10–30% if the fire area exceeds 1600 cm^2 (at 800 K) or 4000 cm^2 (at 500 K).

A flight altitude of 3000 m above ground level was selected for the ABAS overpasses of the fire test site on 23 August 2001.



Figure 3. ABAS sensor platform.



Figure 4. ABAS controller rack.

Table 3. ABAS characteristics.

Parameter	Channel	Figures
Spectral range	VIS/NIR ¹	0.40–0.59 μm
	MWIR	3.4–4.2 μm
	TIR	8.5–9.3 μm
Field of view (FOV)	VIS/NIR	80°
	MWIR/TIR	19°
Detector elements number (no. of pixels/line)	VIS/NIR	5184
	MWIR/TIR	2 × 512 (staggered)
Instantaneous field of view	VIS/NIR	0.32 mrad
	MWIR/TIR	0.65 mrad
Specified noise equivalent temperature difference (°)	MWIR	0.5 K
	TIR	0.3 K

¹The WAAC is a three line CCD stereo scanner with a changeable entrance filter.

6. Fire experiment preparation and weather data records

The Fire Ecology Research Group and a team of the German Weather Service (DWD) tested the conditions for controlled burning of the selected fire plots several times per day starting from 19 August 2001. The weather at that time was a mix of

Table 4. Typical ABAS swath widths and pixel sizes.

Flight altitude over ground (m)	Swath width (m)		Linear pixel size (m)	
	VIS/NIR	MWIR/TIR	VIS/NIR	MWIR/TIR
2000	~3300	~660	~0.7	~1.4
3000	~5000	~1000	~1.0	~2.0
4000	~6600	~1320	~1.4	~2.8

sunshine and rain. Therefore, several days were necessary to dry the forest substantially.

Weather data (temperature, relative humidity, wind speed) were recorded in 15-second intervals at 0.35 m and 2.0 m height before and during the fire experiment on a site covered by grass, located 30 m apart from Plot IV. On the experimental day the German Weather Service issued Forest Fire Danger Class II warning.

Fine fuel moisture content was measured before and during the fire experiment. In the afternoon of 22 August the fire fuel content was 24.5%, followed by a rise to 32.1% during the night and a decrease to 9% in the afternoon of 23 August at the time of burning. This value corresponds to Forest Fire Danger Class IV for surface fires.

Table 5 summarizes the most important fuel and weather parameters at the time of the experiment.

The overpass of ABAS on the 'Aero Commander' aircraft was scheduled for 23 August 2001, 16:00 h local time (UTC + 2 hours).

It was decided to burn Plot IV at a time and with ignition sequences that allowed several ABAS data record overpasses. The ignition times of the four plots are given in table 5.

7. Fire experiment scenario, ABAS records, and *in situ* measurements

The following fire scenarios were realized as the aircraft with ABAS arrived over the test-site at 16:06 h:

- Plot I, ignited at 13:45 h, and only partly extinguished by the LAUBAG fire brigade at 14:30 h, showed small weak burning areas.
- Plot II, ignited at 14:43 h was still burning and contained major hot areas (this plot was not extinguished by the fire brigade at all). Figure 5 shows a part of the Plot II after ignition.
- Plot IV was ignited at 15:58 h in its middle part from the north-east and the fire was growing. Figure 6 shows one part of the burning plot.

Several ABAS data records were conducted from an altitude of 3 km in the period from 16:06 to 16:40 h, the northern part of Plot IV was ignited from north-east at 16:10 h, and the southern part of Plot IV was ignited from north-east at 16:30 h. Plot III was ignited at 17:45 h, i.e. one hour after the last ABAS data acquisition no. 6.

The flame length, the rate of spread, the fire temperature on several levels above ground and other parameters of the burning plots were measured. Figure 7 shows the flame lengths as observed on ground for Plots I–IV. Figure 8 shows the rate of spread (V) of the main fire front of the four fire plots.

Fire temperatures were recorded at the surface of the mineral soil and at different

Table 5. The most important parameters of fuel (fuel moisture) and weather conditions (air temperature, relative humidity, wind speed (minimum, mean and maximum) at 35 cm height).

Plot #	Time of ignition	Fuel moisture content (%)					Air temperature (°C)	Relative humidity (%)	Wind speed (m s ⁻¹)
		Grass (dead)	Grass (green)	Timelag classes					
				1	10	100			
I	13:45	28	100	9.7	12.8	13.0	28	44	0.5–0.8–1.3
II	14:43						29	42	0.7–1.0–1.4
III	17:54						25	47	0.6–1.0–1.3
IV	15:58						29	44	0.5–0.9–1.3



Figure 5. A part of the forest fire in Plot II after ignition.



Figure 6. Part of the burning Plot IV.

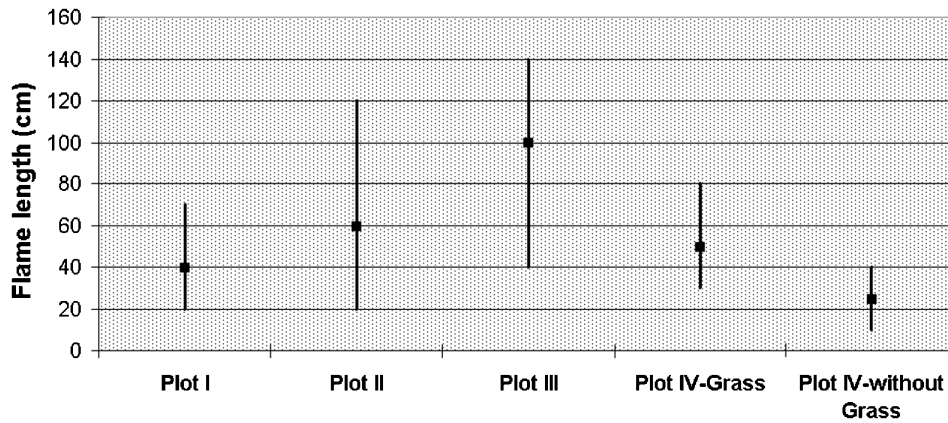


Figure 7. Flame lengths (minimum, mean and maximum) of the fire fronts as observed on ground for Plots I–IV.

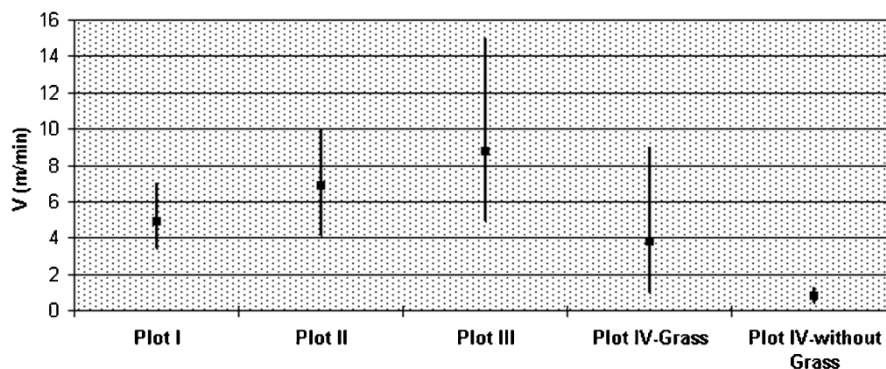


Figure 8. Rate of spread (V) of the main fire front with the four experimental plots. (Plot IV has been subdivided by observations of sites with and without grass cover.)

heights above the mineral soil (5, 30 and 50 cm). Figure 9 shows the temperatures recorded by thermocouples and a data logger in Plots I and II.

The equipment for the measurement of the fire temperature in Plot IV was unfortunately destroyed during the burning, but the flame length, the rate of spread, the fire temperature of Plot II and Plot IV are comparable.

8. Fire map analysis: results and discussion

The ABAS data obtained during six data records conducted over the test site on 23 August 2001 were pre-processed, screened, and calibrated (for several overpasses) to verify the thermal mapping capability of ABAS with special regard to fires.

Figure 10 shows image fragments from the burning Plots I, II and IV that were obtained during ABAS record B. In the VIS image (figure 10(a)), smoke is clearly seen over the actively burning Plot IV, while practically no significant smoke can be recognized over Plots I and II, which were ignited several hours previously. The MWIR image (figure 10(b)) shows all three burning plots (I, II, and IV) as extended hot events. These hot events are also well pronounced in the TIR image (figure 10(c)),

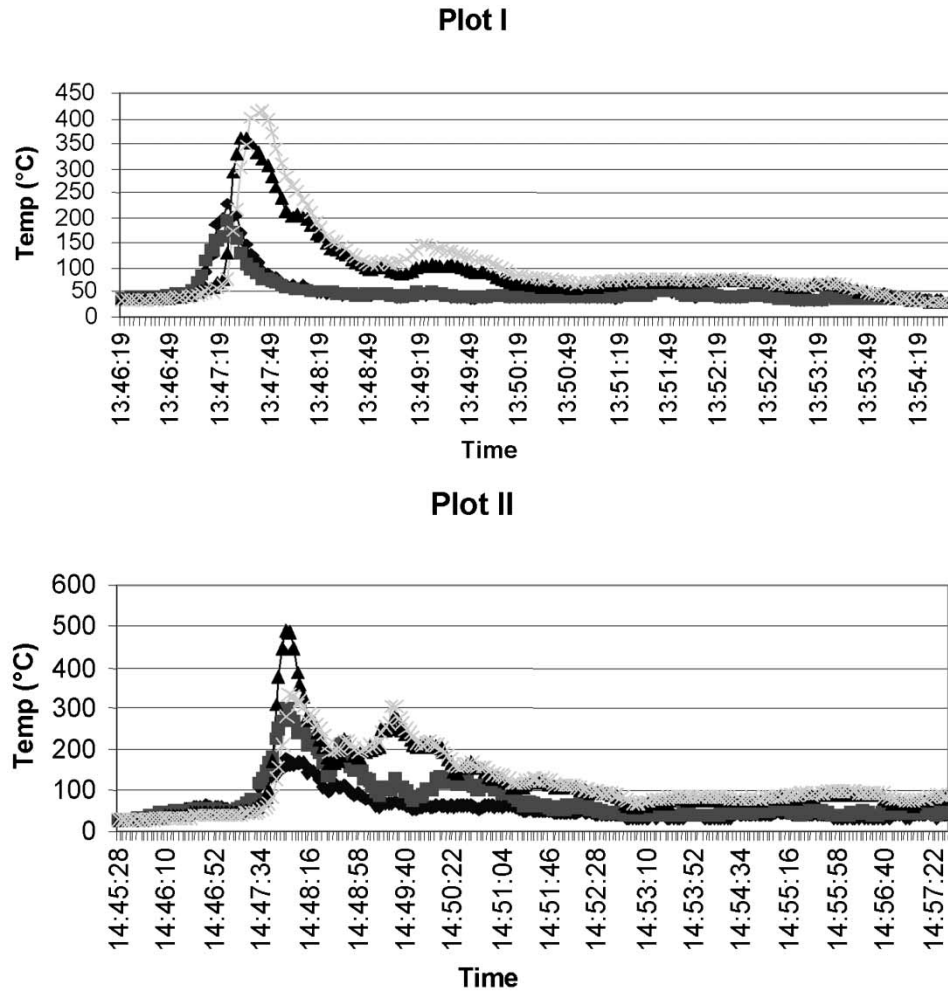


Figure 9. Temperatures recorded by thermocouples and a data logger in Plots I and II.

but here their contrast to the background is lower than in the MWIR and some 'colder' areas can be also recognized within the burning plots.

In these images, the normal temperature background is given in black and white, where black corresponds to 290 K and white to 320 K. For temperatures above 320 K, colour coding is used.

The maximum values of the MWIR pixel-averaged temperatures (figure 10(b)) are:

- 570 K for Plot I, which was a weak smouldering fire at 16:40 h;
- 620 K for Plot II, already a smouldering fire that time; and
- 630 K for the partly flaming fire Plots IVa and IVb.

The maximum values of the TIR pixel-averaged temperatures (figure 10(c)) are:

- ~400 K for Plot I;
- ~450 K for Plot II; and
- > 500 K for partly flaming Plots IVa and IVb.

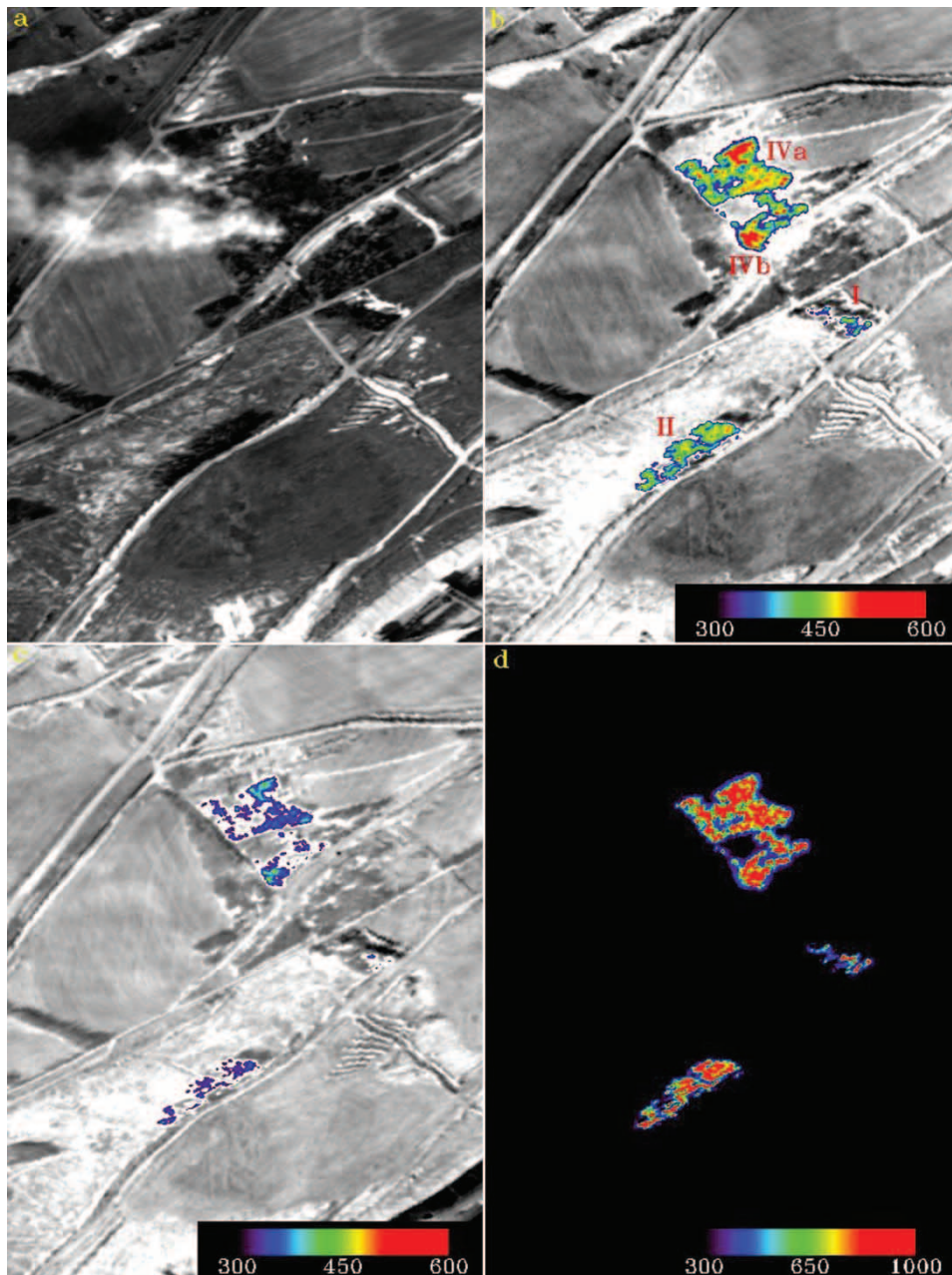


Figure 10. Image obtained by ABAS during Record **B**: (a) VIS; (b) MWIR; (c) TIR; (d) effective fire temperature distribution. Colour-coding is used to represent the high temperature ranges in (b)–(d). The normal temperature background is given in black and white where black represents 290 K and white 320 K.

Even the ABAS $2\text{ m} \times 2\text{ m}$ pixels, occupied by fire, are a complex mixture of burning woody material, charred and unburned vegetation (e.g. not inflamed canopies), resulting in sub-pixel mixtures of various temperatures.

The fact that the MWIR pixel-averaged temperatures of the mixed fire pixels are significantly higher than their TIR pixel-averaged temperatures is explained by the non-homogeneity of these pixels and the higher fire contribution to the pixel signal in the MWIR band than in the TIR band. Furthermore, the mean pixel temperatures are significantly lower than typical fire temperatures measured on ground—as shown, for instance, for Plots I and II in figure 9.

A method to estimate an effective burning temperature in the sub-pixel domain is provided by the bi-spectral technique (Dozier 1981). It is based on using pixel-averaged MWIR and TIR radiances to retrieve two parameters: an effective fire temperature and an effective relative fire area in a pixel. In fact, these parameters of an equivalent homogeneous fire over a constant background would produce the same pixel-averaged MWIR and TIR radiances as the actual non-homogeneous fire. The spatial distribution of this effective fire temperature is shown in figure 10(d). It illustrates a very non-homogeneous distribution of burning in the plots.

Unfortunately, retrieval of the effective fire temperature and area at the pixel level is very sensitive to relative geometrical shifts and the difference of the point spread functions (PSF) of the MWIR and TIR channels, as well as to the background radiance estimation (especially in the TIR channel) (Zhukov and Oertel 2001). Therefore, the fire temperature distribution in figure 10(d) should be interpreted in a qualitative rather than in a quantitative way.

There is significantly higher stability in fire temperature and area retrieval in the cases where bi-spectral analysis is applied to entire fire plots, since this allows errors to be avoided due to inter-channel miss-registration and PSF difference (Zhukov and Oertel 2001). For this reason, the ABAS HSRS data of the entire Plots I and II were used, while Plot IV was divided in two parts: Plot IVa where the burning started 20 minutes earlier and Plot IVb where the burning started just before Record A.

The effective fire temperature and the ‘summarized’ fire area for the burning plots are compared in table 6 for Records A and B, which were taken with an interval of 9 min. The effective fire temperature of 800–900 K is typical for active burning. A decrease of the effective fire temperature in the time interval between the data records took place for Plot I where only small residual burning was left after the fire was extinguished. A significant decrease of the effective burning area is evident for Plot II, where the fire was decreasing by itself. While in Plot IVa the burning is practically stable, fire development in the recently ignited Plot IVb leads to an increase of the effective fire temperature and a significant increase of the effective fire area between the data records.

Table 6. Effective fire parameters for the burning Plots I, II, IVa and IVb.

ABAS record	Plot I	Plot II	Plot IVa	Plot IVb
Record A (at 16:34 h):				
Effective temperature (K)	872	909	871	869
Effective area (m ²)	3.5	35	82	18
Energy release (MW)	0.11	1.3	2.6c	0.58
Record B (at 16:43 h):				
Effective temperature (K)	816	906	863	909
Effective area (m ²)	3.1	20	86	32
Energy release (MW)	0.077	0.76	2.7	1.2

The effective fire temperature as defined from the ABAS data is 100–200 K higher than obtained from the on-ground temperature measurements during the fire front passes (figure 9). This may be explained by the effect of the high-temperature burning in the canopy layers above 0.5 m (the maximal height of the on-ground sensors).

Another useful parameter for characterization of the biomass combustion rate and the amount of gaseous and particulate emissions of a fire is its radiative energy release (Kaufman *et al.* 1998, Wooster *et al.* 2001). Energy release estimation is more stable than the estimation of the effective fire temperature and area. The energy release distribution in a fire is approximately proportional to the fourth power of the MWIR temperature (Kaufman *et al.* 1998) and therefore its distribution is also characterized by the MWIR image in figure 10(b). The total energy release of the plots is given in the last row of table 6. It confirms decrease of burning in Plots I and II between ABAS overflights **A** and **B**, stable burning in Plot IVa and fire development in Plot IVb.

9. Conclusion and outlook

The first ABAS forest fire flight experiment conducted in the Cottbus region on 23 August 2001 allows us to conclude the following.

The BIRD Hot Spot Recognition System (HSRS), as operated in the ABAS (and later on the BIRD satellite) is able to map simultaneously in the 3.9 μm and in the 8.8 μm bands:

- high temperature events (HTE) leading to ‘apparent pixel temperatures’ of up to 600 K without any saturation effects; and
- normal temperature phenomena of 300 K with a Noise Equivalent Temperature Difference (NE Δ T) of <0.3 K.

These features permit the application of the bi-spectral method (Dozier 1981) to the co-registered HSRS data to retrieve the effective area and effective temperature of HTE—such as forest fires, coal seam fires or volcanic activities—from the acquired pixel averaged radiances.

The HSRS—developed, manufactured and tested by the DLR Institute of Space Sensor Technology and Planetary Exploration within the BIRD mission—can be considered as a unique remote sensing tool for quantitative analysis of fires and volcanic events.

The first results obtained at the end of October 2001 during the commissioning phase of the BIRD mission show a normal function of the HSRS in space. This would allow the investigation of HTE phenomena on Earth without channel saturation and a spatial resolution of 360 m (compared to ~ 1 km resolution of the AVHRR and MODIS MWIR/TIR channels).

Operated on a research aircraft, the ABAS-HSRS may be successfully used for:

- detailed physical characterization of vegetation and coal seam fires, volcanic lava and pyroclastic flows, and geothermal anomalies;
- validation of wildfire data obtained simultaneously by satellite sensors; and
- provision of spatially high resolution ‘classifying’ image data to be combined with spectrally high resolution data of a nadir looking fast scanning/profiling IR Fourier-Transform (IR-FT) spectrometer for data fusion and successive retrieval of the HTE emission products.

The last point indicates the combined utilization of ABAS and the fast scanning and very robust IR FT-instrument MIROR (a very fast measuring Michelson Interferometer with ROTating Retroreflectors), which is at the DLR Remote Sensing Technology Institute (Haschberger and Tank 1993), on one aircraft. This will be the new airborne facility Fire Airborne Simulator Arrangement (FASA). Most important, however, are the prospects to meet the requirements of the users of remote sensing information in fire management. The ability of the HSRS to discriminate a broader range of background and fire temperatures before reaching saturation has an innovative potential. For instance, regularly occurring low-intensity surface fires in extended forest areas of the boreal zone burn at lower temperatures and are essential for reducing fuel loads, thus reducing the likelihood of occurrence of high-intensity and high-severity fires (Goldammer and Furyaev 1996). These low-temperature fires must be discriminated from high-intensity fires that burn at higher temperatures and that must be controlled in order to reduce ecosystem damages and economic losses. In remote and largely inaccessible areas of the boreal zone, e.g. in the Russian Federation, remote sensing tools are needed to support decision-making in forest fire management. The first tests of the HSRS confirm that this tool is a candidate to distinguish ecologically beneficial low-intensity fires from destructive fires burning at higher temperatures.

Appendix. List of abbreviations

ABAS	Advanced BIRD Airborne Simulator
ARINC	Airborne inertial data
AVHRR	Advanced Very High Resolution Radiometer
AWFS	Automatisches Waldbrand Frühwarn System (German), Automated System for Early Forest Fire Detection
BAS 1	BIRD Airborne Simulator no. 1
BIRD	Bi-spectral Infrared Detection
CCD	Charge coupled device
CMT	Cadmium mercury telluride
DFNK	Deutsches Forschungsnetz für Naturkatastrophen
*ESA	European Space Agency
FASA	Fire Airborne Simulator Arrangement
FEMAS	Fire Emission Assessment System
FOV	Field of view
GFMC	Global Fire Monitoring Center
GIS	Geo Information System
GPS	Global Positioning System
HSRS	Hot Spot Recognition System
*H/W	Hardware
HTE	High temperature events
*IFOV	Instantaneous field of view
*INS	Inertial Navigation System
IR	Infrared
IR-FT	Infrared-Fourier Transform spectrometer
LAUBAG	Lausitzer Bergbau Aktien Gesellschaft
MIROR	Michelson Interferometer with Rotating Retroreflector
MWIR	Mid wave infrared

NETD	Noise Equivalent Temperature Difference
*NESR	Noise Equivalent Spectral Radiance
NIR	Near infrared
PSF	Point spread function
*SCSI	Small Computer Standard Interface
SNR	Signal to noise ratio
*S/W	Software
TIR	Thermal infrared
VIS	Visible
WAAC	Wide angle airborne camera
WAOSS	Wide angle optoelectronic stereo scanner

References

- ARINO, O., and MELINOTTE, J. M., 1998, The 1993 Africa fire map. *International Journal of Remote Sensing*, **19**, 2019–2023.
- AHERN, F. J., GOLDAMMER, J. G., and JUSTICE, C. O. (editors), 2001, *Global and Regional Vegetation Fire Monitoring from Space: Planning a coordinated international effort* (The Hague: SPB Academic Publishing).
- CAHOON, JR, D. R., STOCKS, B. J., LEVINE, J. S., COFER, III, W. R., and O'NEIL, K. P., 1992, Seasonal distribution of African savanna fires, *Nature*, **359**, 812–815.
- DEEMING, J. E., BURGAN, R. E., and COHEN, J. D., 1977, The National fire-danger rating system—1978. Forest General Technical Report INT-39, United States Department of Agriculture, USA.
- DFNK (DEUTSCHES FORSCHUNGSNETZ NATURKATASTROPHEN), 2001, German Research Network of Natural Disasters. <http://www.dfkn.de>.
- DOZIER, J., 1981, A method for satellite identification of surface temperature fields of sub-pixel resolution. *Remote Sensing of Environment*, **11**, 221–229.
- FIRE, 1994, Fire Recognition System for Small Satellites, Phase A Study. DLR Institute of Space Sensor Technology, Berlin and OHB-System, Bremen, Germany.
- FLANNIGAN, M. D., and VON DER HAAR, T. H., 1986, Forest fire monitoring using NOAA satellite AVHRR. *Canadian Journal of Forest Research*, **16**, 975–982.
- FLASSE, S. P., and CECCATO, P., 1996, A contextual algorithm for AVHRR fire detection. *International Journal of Remote Sensing*, **17**, 419–424.
- FRANCA, J. R. A., BRUSTET, J. M., and FONTAN, J., 1995, Multispectral remote sensing of biomass burning in West Africa. *Journal of Atmospheric Chemistry*, **22**, 81–110.
- GFMC (Global Fire Monitoring Center), 2001, <http://www.uni-freiburg.de/fireglobe/>.
- GIGLIO, L., KENDALL, J. D., and JUSTICE, C. O., 1999, Evaluation of global fire detection using simulated AVHRR infrared data. *International Journal of Remote Sensing*, **20**, 1947–1985.
- GIGLIO, L., and KENDALL, J. D., 2001, Application of the Dozier retrieval to wildfire characterization—a sensitivity analysis. *Remote Sensing of Environment*, **77**, 34–49.
- GOLDAMMER, J. G., and FURYAEV, V. V. (editors), 1996, *Fire in Ecosystems of Boreal Eurasia* (Dordrecht: Kluwer Academic Publishers).
- HASCHBERGER, P., and TANK, V., 1993, Optimization of a Michelson Interferometer with a rotating retroreflector in optical design, spectral resolution, and optical throughput. *Journal of the Optical Society of America A*, **10**, 2338–2345.
- JUSTICE, C. O., KENDALL, J. D., DOWTY, P. R., and SCHOLLES, R. J., 1996, Satellite remote sensing of fires during the SAFARI campaign using NOAA advanced very high resolution radiometer data. *Journal of Geophysical Research*, **101**, 23851–23863.
- KAUFMAN, Y. J., TUCKER, C. J., and FUNG, I., 1990, Remote sensing of biomass burning in the tropics. *Journal of Geophysical Research*, **95**, 9927–9939.
- KAUFMAN, Y. J., JUSTICE, C. O., FLYNN, L. P., KENDALL, J. D., PRINS, E. M., GIGLIO, L., WARD, D. E., MENZEL, W. P., and SETZER, A. W., 1998, Potential global fire monitoring from EOS-MODIS. *Journal of Geophysical Research*, **103**, 32 215–32 238.

- KÜHRT, E., BEHNKE, T., JAHN, H., HETZHEIM, H., KNOLLENBERG, J., MERTENS, V., SCHLOTZHAUER, G., and GÖTZE, B., 2000, Autonomous early warning system for forest fires tested in Brandenburg (Germany). *International Forest Fire News*, **22**, 84–90. http://www.uni-freiburg.de/fireglobe/iffn/country/de/de_6.htm.
- LEE, T. F., and TAG, P. M., 1990, Improved detection of hotspots using the AVHRR 3.7- μ m channel. *Bulletin of the American Meteorological Society*, **71**, 1722–1730.
- LI, Z., CIHLAR, J., MOREAU, L., HUANG, F., and LEE, B., 1997, Monitoring fire activities in the boreal ecosystem. *Journal of Geophysical Research*, **102**, 29 611–29 624.
- PEREIRA, M. C., and SETZER, A. W., 1993, Spectral characteristics of deforestation fires in NOAA/AVHRR images. *International Journal of Remote Sensing*, **14**, 583–597.
- POZO, D., OLMO, F. J., and ALADOS-ARBOLEDAS, L., 1997, Fire detection and growth monitoring using a multitemporal technique on AVHRR mid-infrared and thermal channels. *Remote Sensing of Environment*, **60**, 111–120.
- PRINS, E. M., and MENZEL, W. P., 1992, Geostationary satellite detection of biomass burning in South America. *International Journal of Remote Sensing*, **13**, 2783–2799.
- PRINS, E. M., FELTZ, J. M., MENZEL, W. P., and WARD, D. E., 1998, An overview of GOES-8 diurnal fire and smoke results for SCAR-B and 1995 fire season in South America. *Journal of Geophysical Research*, **103**, 31 821–31 835.
- RANDRIAMBELO, T., BALDY, S., BESSAFI, M., PETIT, M., and DESPINOY, M., 1998, An improved detection and characterization of active fires. *International Journal of Remote Sensing*, **19**, 2623–2638.
- RAUSTE, Y., HERLAND, E., FRELANDER, H., SOINI, K., KUOREMÄKI, T., and RUOKARI, A., 1997, Satellite-based forest fire detection for fire control in boreal forests. *International Journal of Remote Sensing*, **18**, 2041–2656.
- ROBINSON, J. M., 1991, Fire from space: global fire evaluation using infrared remote sensing. *International Journal of Remote Sensing*, **12**, 3–24.
- SKRBEK, W., and LORENZ, E., 1998, HSRS—an infrared sensor for hot spot detection. *Proceedings of the SPIE*, **3437**, 167–175.
- WOOSTER, M. J., ZHUKOV, B., and OERTEL, D., 2001, Fire radiative energy for quantitative study of biomass burning: derivation from the BIRD experimental satellite and comparison to MODIS fire products. *Remote Sensing of Environment*, in press.
- ZHUKOV, B., and OERTEL, D., 2001, Hot Spot Detection and Analysis Algorithm for the BIRD Mission. Algorithm Theoretical Basic Document (ATBD), DLR, Berlin, Germany.